

SCIENTIFIC REPORTS

OPEN

High-throughput SRCD using multi-well plates and its applications

Rohanah Hussain, Tamás Jávorfí, Timothy R. Rudd[†] & Giuliano Siligardi

Received: 08 April 2016
Accepted: 03 November 2016
Published: 22 December 2016

The sample compartment for high-throughput synchrotron radiation circular dichroism (HT-SRCD) has been developed to satisfy an increased demand of protein characterisation in terms of folding and binding interaction properties not only in the traditional field of structural biology but also in the growing research area of material science with the potential to save time by 80%. As the understanding of protein behaviour in different solvent environments has increased dramatically the development of novel functions such as recombinant proteins modified to have different functions from harvesting solar energy to metabolomics for cleaning heavy and metal and organic molecule pollutions, there is a need to characterise speedily these system.

Circular Dichroism (CD) is the differential absorption between left and right circularly polarized light of a chiral molecule, which is not super-imposable to its mirror image. CD spectroscopy is sensitive to the absolute configuration and conformation of chiral molecules.

Recent theoretical advances in *ab initio* calculations using time-dependent density functional theory (TD-DFT)¹ has enabled an unprecedented improvement of the assignment of the absolute configuration of chiral molecules in terms of quality and easiness far superior than any other method including X-ray crystallography. For macromolecules such as proteins under a given environmental condition, the far-UV CD signal reflects the content of the secondary structure elements such as α -helix, β -strand, β -turns, collagen type (PPII) and unordered structure that can be estimated quantitatively using the most popular CONTIN, SELCON and CDSSTR methods²⁻⁵.

In this article, we will focus on the application of CD spectroscopy to proteins as they will continue to dominate the biomedical research area for the foreseeable future^{6,7}. High-throughput assays using multi-plates are routinely used in crystallisation, biological activity, drug screening, and protein stability assays through radiolabelled immuno assays, UV-Vis absorption, fluorescence quenching, and surface plasmon resonance techniques⁸⁻¹⁰. Unsuccessful attempts were made in the 90's to measure the CD of samples in multi-well plates (Castiglioni, Jasco Europe, personal communication). Apart from the distortion that can be generated by the meniscus of the solution in the well, there is an intrinsic problem due to the depolarisation of the incident light being deflected by a 45° grazing angle mirror in the sample chamber in order for the light to be transmitted through each of the 96- or 384- wells of the horizontally laid multi-well plates. This is the main reason why CD spectroscopy has been done using individual cuvettes.

However, this is not the case with Diamond B23 beamline for synchrotron radiation circular dichroism (SRCD) where the recently developed vertical sample chamber can accommodate the 96- and 384-well multi-well plates held on an X-Y motorised stage (Prior) (Fig. 1a,b). Inside the chamber, the monochromatic incident light is reflected upwards at right angle by a plane mirror, which is located before the device (a combination of a Rochon polariser-prism and a photo elastic modulator (PEM) (Hinds)) that generates the left and right circularly polarised light with 50 kHz modulation. With this arrangement we can eliminate the problem of depolarisation, observed earlier using bench-top CD instruments, by optical elements that are placed behind the PEM.

One of the unique feature of Diamond B23 beamline for SRCD is the highly collimated light beam (about 0.5 mm (H) \times 0.3 mm (V) FWHM), which has been exploited for measurement of samples with limited availability using small aperture cells of low volume capacity (from 40 μ l for 1 cm to 800 μ l for 10 cm pathlengths)¹¹⁻¹³. This feature also enabled the measurement to be conducted on the centre of each well of a multi-plate without any significant distortion effect produced by the meniscus of the liquid (Fig. 1e). For both 96- and 384-well multi-plates, this was verified by scanning the base area of the well by moving the motorised X-Y stage in a rastering manner in 0.5 mm steps and recording the SRCD spectrum of aqueous (1 S) (+) 10-camphorsulfonic acid (CSA) for each step point (Fig. 1f,g). The SRCD spectra showed the distortion of the CSA spectrum due to the meniscus when

Diamond Light Source, Diamond House, Chilton, Didcot OX11 0DE, United Kingdom. [†]Present address: National Institute for Biological Standards and Control (NIBSC), Blanche Lane, South Mimms, Potters Bar, Hertfordshire, EN6 3QG, England. Correspondence and requests for materials should be addressed to R.H. (email: rohanah.hussain@diamond.ac.uk) or G.S. (email: giuliano.siligardi@diamond.ac.uk)

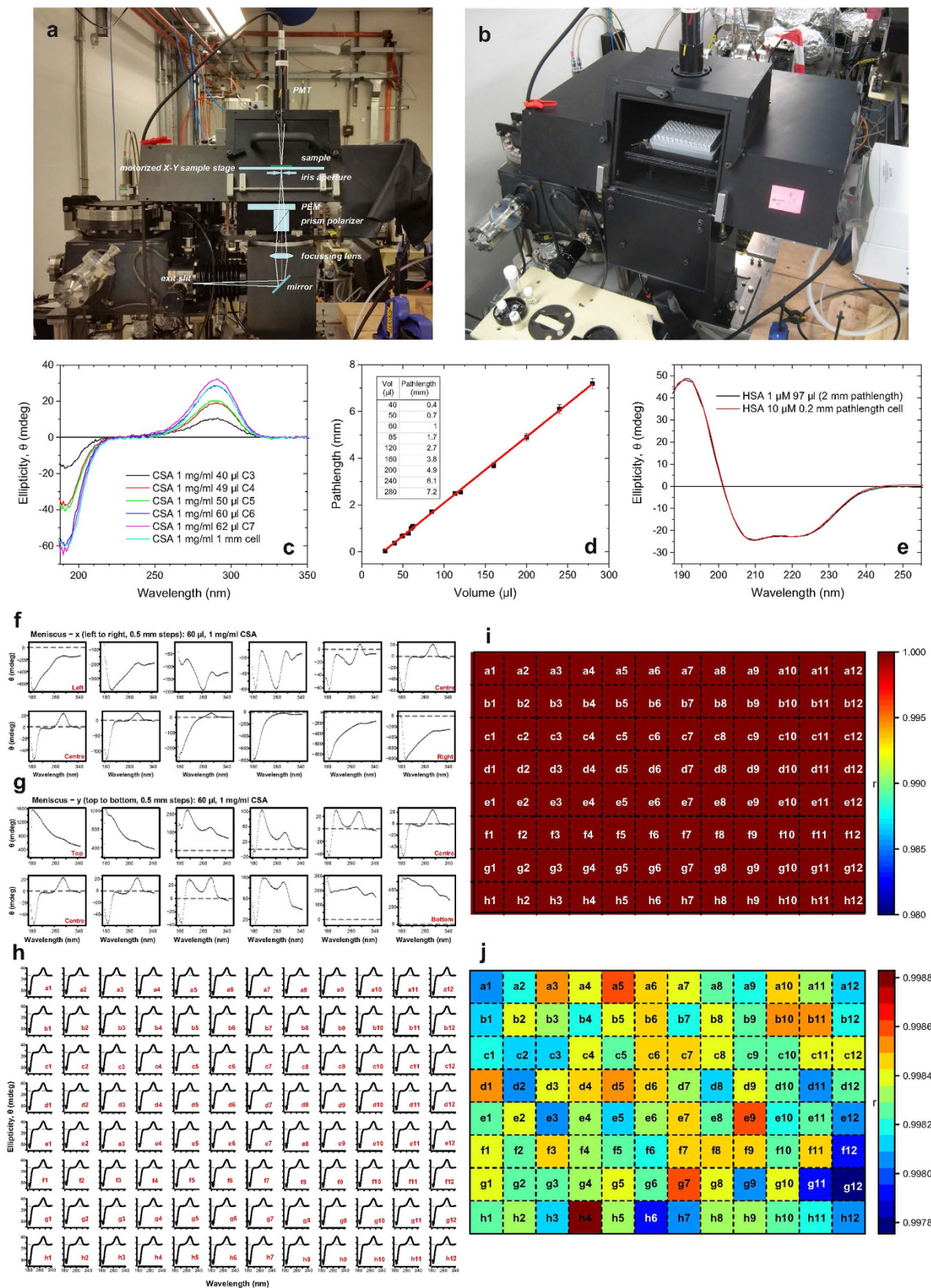


Figure 1. (a) Sketch of the optical elements superimposed to the picture of the vertical chamber unit (exit slit, 45° plane mirror, focusing lens, polariser prism, PEM (photo elastic modulator), iris, X-Y motorised stage, horizontal sample and PMT (photo multiplier tube) detector). The sample is placed on the motorised X-Y stage (b) Picture with the open door of the vertical chamber showing the 96-well plate held in on the X-Y motorised stage. (c) SRCD spectra of CSA aqueous solution (1 mg/ml) in 96-well plate measured with the vertical chamber for HT-SRCD. The spectra illustrate the different pathlengths achieved for the pipetted volumes between

40 μ l to 62 μ l compared to the spectrum measured with 1 mm pathlength cell as the reference. Note that the spectrum with 60 μ l volume is completely superimposed to that of the 1 mm pathlength cell. **(d)** Linear Correlation found between the pathlength and the volume aliquots of CSA in the 96-well multiplate ($y = a + bx$; $R^2 = 0.99925$). Insert is a table summarising the equivalent pathlengths for a set of volumes. **(e)** SRCD spectrum of 97 μ l of human serum albumin (HSA) 1 μ M pipetted into the well is compared to that of 10 μ M HSA measured in a 0.02 cm cell pathlength (Hellma). The spectra were identical confirming that the equivalent pathlength of the well with 97 μ l was indeed 2 mm. **(f)** Spectral distortions induced by the meniscus when the incident beam was not passing through the centre of the well in the x-axis. **(g)** Spectral distortions induced by the meniscus when the incident beam was not passing through the centre of the well in the y-axis. **(h)** SRCD spectra of CSA in each of the 96-well plate. **(i)** Correlation between CD spectra of 96-well plate with 60 μ l volume in each well and CSA average plate well spectrum with correlation scale from 0 to 1. **(j)** Correlation between CD spectra of 96-well plate with correlation within 0.2%

the light beam did not pass through the centre of the well (Fig. 1f,g). Once the multi-plate was aligned with the light beam passing through the central position of the first well (A1 coordinate), the movement of the X-Y stage to the next centre of the adjacent well was controlled in a rastering manner via script to auto-measure the 96 SRCD spectra. Sample position from scan to scan error were carried out by running CSA measurement on each of the 96 wells of the multi-plate as reported in Fig. 1h. Correlation analysis showed the 96 well CSA measurements gave a 0.2% deviation from the average CSA well spectrum (Fig. 1i,j) well within the limits of reproducible spectra. In the followings we describe the first HTCD data obtained using the newly developed vertical sample chamber of B23 beamline for SRCD.

Methods and Materials

The modular vertical chamber for 96- or 384-well multiplate can be accommodate in both B23 module stations A and B (Fig. 1). B23 was calibrated with an aqueous solution of CSA 1 mg/ml in a 1 mm pathlength cell as the standard CD reference¹⁴. Different volumes of the 1 mg/ml CSA solution were transferred in the 96-well multiplate to calculate the various equivalent cell pathlength of the wells (Fig. 1c). For all wells, the CD spectra were recorded in duplicate samples in the 185–350 nm spectral region. Measurements were performed under nitrogen flushed end-station A or B with 1 scan per well, using an integration time of 2 s/data point. Volume-pathlength correlation was calculated using the CD intensity at 290 nm at different volumes of CSA samples and compared with that of the same solution recorded in a fixed 1 mm pathlength cell. Measurements to see the effects of the meniscus were carried out using 60 μ l of CSA 1 mg/ml dispensed into the well, where CD spectra were collected at every 500 μ m step from the top to bottom and left to right along the vertical and horizontal diagonals of the well. The X-Y stage was then set to the centre of the well A1. 60 μ l of CSA 1 mg/ml dispensed into each of the 96-well plate to check for variation in the well to well alignment with respect to the beam (Fig. 1h).

Several solid protein samples were weighed and proteins solutions were prepared at a concentration of 0.8–2.5 mg/ml depending on the extinction coefficient of the proteins for absorption of 1 at 280 nm in a 0.5 cm pathlength cell. These concentrations were used for the near-UV SRCD measurements. However, for the far-UV SRCD measurements, the proteins were diluted to 0.05–0.1 mg/ml and 60 μ l of protein samples were loaded into the 96-well (6.6 mm diameter well) in duplicate or triplicate. For the near UV measurements the proteins samples were loaded with 200 μ l of samples in duplicate or triplicate on the 96-well. Equivalent amount of 10 mM phosphate buffer of 60 μ l and 200 μ l were loaded onto the 96-well as buffer baseline measurements for baseline subtraction for far UV (60 μ l) and near UV (200 μ l) HT-SRCD measurements. The multi-well plate is then covered with a quartz coverslip and placed in the vertical chamber for CD measurements. Care should be taken in baseline subtraction by using the same corresponding well where the sample is loaded to avoid any differences in birefringence between the wells which could affect the results. All SRCD measurements were baseline subtracted and processed using CDApps¹⁵.

The multi-well plates can be washed using Hellmanex™ and rinsed with double distilled water and finished off with ethanol 96% to facilitate drying of the plate. The dried multi-well plate can then be re-used by the next users.

Results and Discussion

The results showed in Fig. 1c varying CD signal which corresponds to different volume of CSA used. This can also be achieved varying the concentration and the volume used. Using the results from these measurements, a plot of CD datapoint taken at 290 nm showed a good linear relationship giving rise to the corresponding pathlength for a specific volume of solution (Fig. 1d). The results obtained showed that the CSA reference sample measurements were reproducible and the multi-well plate sample chamber compartment was the crucial key to the success of HT-SRCD. Comparative SRCD spectrum of 97 μ l (equivalent to 2 mm pathlength) of HSA 1 μ M was also found to be superimposable with the SRCD spectrum of 10 μ M of HSA in 0.2 mm fixed pathlength cell (Fig. 1e).

The position of the centre of each well of the 96 multi-well plate was measured using a 3D coordinate laser tracker (Leica AT401 with point to point accuracy of 10 μ m) to assess for any imprecision and misalignment that could potentially introduce distortions to the CD spectra of the wells due to the meniscus effect. The differences between the theoretical and observed coordinates of the centre of each of the 96 wells ($12 \times 8 = 96$ wells at 9.000 mm apart horizontally and vertically from one each other) were within 50 microns ruling out any possible distortions observed in Fig. 1f,g once the central position of a well taken as reference was established. HT-CD measurements of the CD standard aqueous CSA of the multi-plate after alignment calibration showed that the variation of CD spectra among the 96 wells compared to the average CSA CD well spectrum was within 0.2% well below the error limit of reproducible CD measurements (Fig. 1h,i,j).

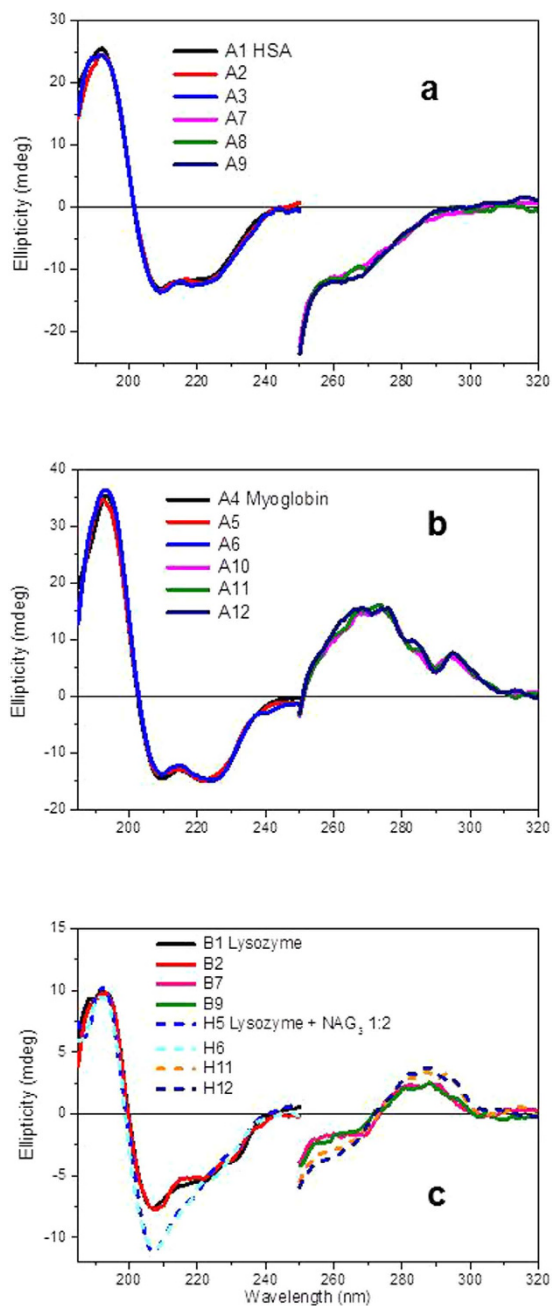


Figure 2. SRCD spectra of proteins measured in PBS 10 mM, pH 7.5 duplicates or triplicates. (a) human serum albumin (HSA), (b) myoglobin and (c) egg white lysozyme with and without ligand NAG₃ (molar ratio 1:2) using Suprasil quartz 96-well microplate (Hellma) with B23 module A for HT-SRCD in both far-UV (60 μ l equivalent to 1 mm pathlength) and near-UV (200 μ l equivalent to 4.9 mm pathlength) regions in different wells.

Based on the volume-pathlength correlation established in Fig. 1d, 60 μ l of 0.05 mg/ml of human serum albumin (HSA) and 0.1 mg/ml of myoglobin respectively were used as reference samples for an equivalent pathlength cell of 1 mm. The SRCD spectra in Fig. 2a,b illustrate the flexibility of the HT-SRCD that can be used to assess conformational behaviour of proteins both in the far-UV region that is characteristic to the protein secondary structure and in the near-UV region where it is sensitive to the local environment of the aromatic amino acid residues¹⁶ and dihedral angle of disulphide bonds¹⁷ as a function of solvent composition, pH, denaturing agents, surfactants and ionic strength².

The detection of ligand binding interactions was also successfully conducted for hen egg white lysozyme protein in the presence of ligand carbohydrate NAG₃ (tri-N-acetyl-D-glucosamine) that is known to bind to lysozyme^{18,19}. In Fig. 2c, the SRCD spectra revealed conformational changes both in the far-UV and near-UV regions upon ligand addition consistent with NAG₃ binding interactions. Secondary structure analysis using CONTIN algorithm^{3,4} showed that there is a loss of 16% of α -helix and a gain of 16% of β -sheet components

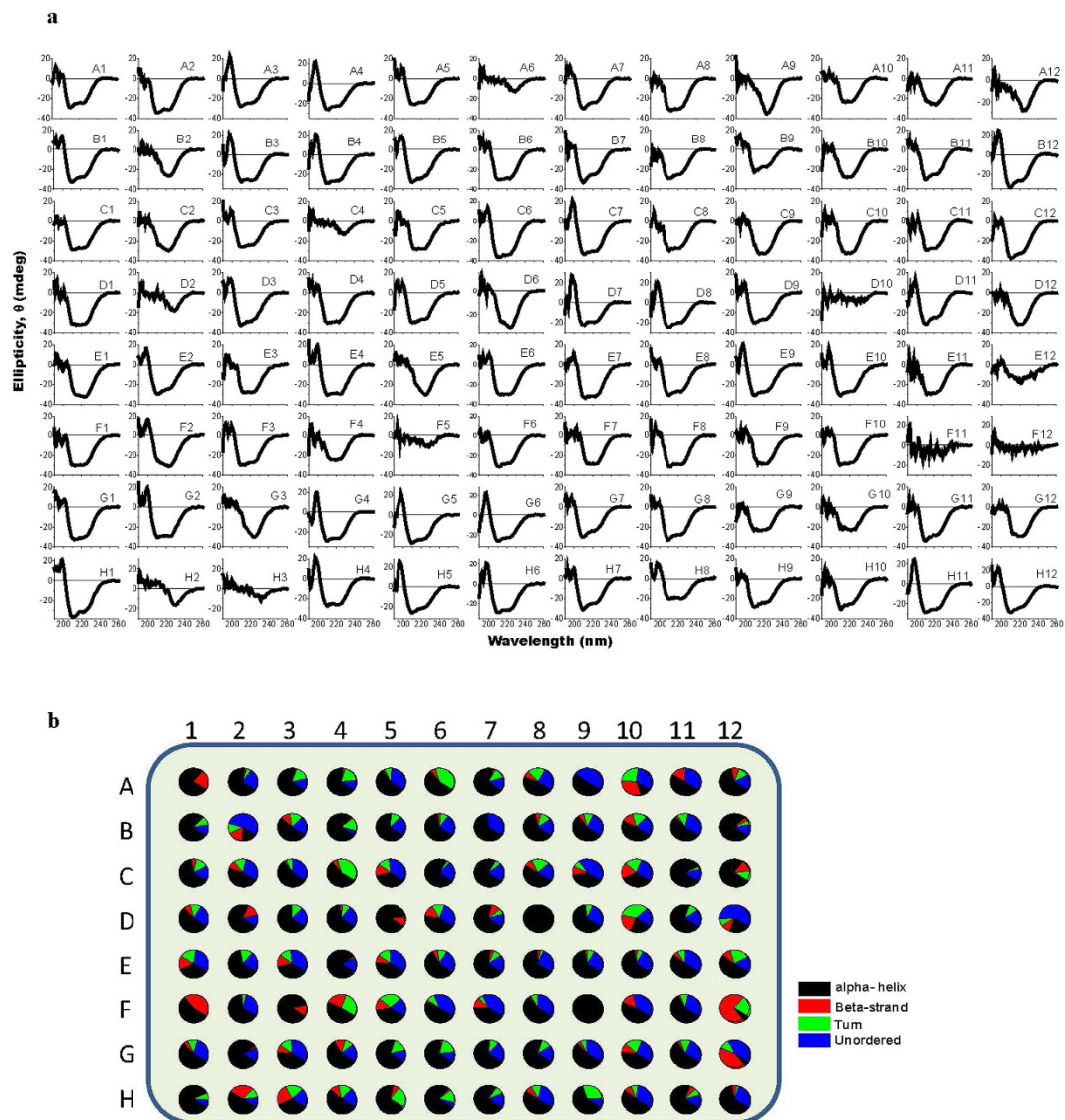


Figure 3. Top, SRCD spectra and below, pie chart of protein secondary structure of myoglobin under 96 different crystallographic “cocktail” conditions. The red boxes highlight the conditions of spectral cut-off at about 230 nm due to too high UV absorption of the solvent.

(normalised mean residual standard deviation, NMRSD 0.05) in lysozyme upon NAG_3 binding. In the near UV region the SRCD changes are only due to the lysozyme Trp residue as it sees the ligand NAG_3 within the 6 Å range of its local environment. CD spectroscopy in the far-UV region indicates directly, unlike other techniques such as ITC, fluorescence and SPR that the ligand, possessing a very small signal, induced a significant conformational change that was unambiguously attributed to the protein.

The first HT-SRCD application of B23 showed that high-throughput measurements can be done using the multi-well system (Fig. 3). In Fig. 3a, the SRCD spectra of the samples has been baseline corrected by subtracting from each sample spectrum the corresponding spectrum of the buffer measured in the same well after a thorough cleaning cycle. Figure 3b illustrates the secondary structure estimation (SSE) from the CD data using CONTIN algorithm^{3,4}. The SRCD screening was conducted on samples of one fifth of the concentration that is usually used for crystallisation conditions. The result shown in Fig. 3b highlights immediately the conformational behaviour of myoglobin as a function of buffer environments; hence it provides valuable information for optimisation of crystallographic conditions. This has implication in the screening application of different system conditions by direct sample transfer to a suprasil type quartz multi-well plate. Varying the volume of the sample solutions transferred into the wells of the multi-well plate enable a broad flexibility of the equivalent pathlength choice that can span from 1 mm to 7 mm range accommodating diluted samples following Beer’s law. Screening applications for conformational changes of biological materials such as proteins and nucleic acids as a function of the environment as well as ligand binding interactions can now be conducted by HT-SRCD.

Conclusions

Further time optimisation by 50% in CD measurement can be achieved by setting up two groups of measurements; one for the far-UV and the other for the near-UV regions. In the far-UV measurements the wavelength range can span from 180 to 260 nm and in the near-UV 250 to 350 nm. This way one can avoid scanning the full wavelength range for each sample which would unnecessarily increase the data acquisition time. Of course this only makes sense for protein samples. With oligonucleotides, however this approach will not work as the region of interest does span the full wavelength range from 180 to 350 nm or even more. Automated CD approach using fixed pathlength²⁰ had not been considered for B23 beamline as the samples are loaded directly to the multi-well plate, hence there is no dead volume involved. Furthermore there is minimal downtime-compared to single cell measurement as cell has to be cleaned in between measurement and sample loading. This is an essential requirement from Users coming to the beamline with limited amount of materials available but with a high number of measurements required as well as defined beamtime allocated which have to be efficiently used. With multi-well plates, good accuracy of micro-pipetting is critical particularly for SRCD measurements where the CD intensity is often small and any error introduced by pipetting can therefore have a significant impact on the data analysis. This is not the case for automated CD measurements with benchtop instruments using fixed pathlength cell²⁰, although there is a high risk of blocking the piping circuit during the cleaning and filling of the cuvette cell when using proteins. For this reason, duplicate measurements using HT-SRCD are recommended in order to minimise errors in sample filling common to all assays and HT techniques.

References

1. Yanan, H. E., Wang, B., Dukor, R. K. & Nafie, L. A. Determination of Absolute Configuration of Chiral Molecules Using Vibrational Optical. *Applied Spectroscopy*. **65**, 699–723 (2011).
2. Fasman, G. D. *Circular Dichroism and the Conformational Analysis of Biomolecules*. (Plenum Press, New York, 1996).
3. Sreerama, N. & Woody, R. W. Estimation of protein secondary structure from circular dichroism spectra: comparison of CONTIN, SELCON and CDSSTR methods with an expanded reference set. *Anal. Biochem.* **287**, 252–260 (2000).
4. Provencher, S. W. & Glockner, J. Estimation of globular protein secondary structure from circular dichroism. *Biochemistry* **20**, 33–37 (1981).
5. Siligardi, G. *et al.* Regulation of Hsp90 ATPase activity by the co-chaperone Cdc37p/p50^{cdc37}. *J. Biol. Chem.* **277**, 20151–20159 (2002).
6. Pellicchia, M. *et al.* Perspectives on NMR in drug discovery: a technique comes of age. *Nat Rev Drug Discov.* **7**, 738–45 (2008).
7. van Stokkum, L. H. M., Spoelder, H. J. W., Bloemendal, M., van Grondelle, R. & Groen, F. C. A. Estimation of protein secondary structure and error analysis from circular dichroism spectra. *Anal. Biochem.* **191**, 110–118 (1990).
8. Schonbrun, E., Abate, A. R., Steinvurzel, P. E., Weitzab D. A. & Crozier, K. B. High-throughput fluorescence detection using an integrated zone-plate array. *Lab Chip*. **10**, 852–856 (2010).
9. Maynard, J. A. *et al.* Next generation SPR technology of membrane-bound proteins for ligand screening and biomarker discovery. *Biotechnology Journal*. **4**, 1542–1558 (2009).
10. Macarron, R. *et al.* Impact of high throughput screening in biomedical research. *Nature Reviews Drug Discovery*, **10**, 188–195 (2011).
11. Jávorf, T., Hussain, R., Myatt, D. & Siligardi, G. Measuring circular dichroism in a capillary cell using the B23 synchrotron radiation CD beamline at Diamond Light Source. *Chirality* **22**, E149–E153 (2010).
12. Hussain, R., Jávorf, T. & Siligardi, G. *Spectroscopic Analysis: Synchrotron Radiation Circular Dichroism. Comprehensive Chirality*. (eds Carreira, E. M. & Yamamoto, H.) Ch. 8, 438–448 (Elsevier, 2012).
13. Hussain, R., Jávorf, T. & Siligardi, G. Circular dichroism beamline B23 at the Diamond light source. *J. Synchrotron Rad.* **19**, 132–135 (2012).
14. Chen, G. C. & Yang, J. T. Two point calibration of circular dichrometer with d-10-camphorsulfonic acid. *Anal. Lett.* **10**, 1195–1207 (1977).
15. Hussain, R. *et al.* CDApps: integrated software for experimental planning and data processing at beamline B23 Diamond Light Source. *J. Synchrotron Rad.* **22**, 465–468 (2015).
16. Strickland, E. H. Aromatic contributions to circular dichroism spectra of proteins. *CRC Crit. Rev. Biochem.* **2**, 113–175 (1974).
17. Siligardi, G., Campbell, M. M., Gibbons, W. A. & Drake, A. F. Conformational analysis of the melanin concentrating hormone by Circular dichroic spectroscopy. Disulphide bridge and aromatic tyrosyl contributions. *Eur. J. Biochem.* **206**, 23–29 (1991).
18. Siligardi, G. & Hussain, R. Biomolecules interactions and competitions by non-immobilised ligand interaction assay by circular dichroism. *Enantiomer* **3**, 77–87 (1998).
19. Siligardi, G., Hussain, R., Patching, S. G. & Phillips-Jones, M. K. Ligand. Ligand and drug binding studies of membrane proteins revealed through circular dichroism spectroscopy. *Biochim Biophys Acta.* **1838**, 34–42 (2014).
20. Fiedler, S., Cole, L. & Keller, S. Automated Circular Dichroism spectroscopy for medium throughput analysis of protein conformation. *Anal. Chem.* **85**, 1868–1872 (2013).

Author Contributions

R.H. and G.S. conceived the study and wrote the manuscript. T.J., R.H. and G.S. developed the HT-CD measurement technique. R.H., T.J. and T.R.R. performed the CD spectral measurements. All authors discussed the results.

Additional Information

Competing financial interests: The authors declare no competing financial interests.

How to cite this article: Hussain, R. *et al.* High-throughput SRCD using multi-well plates and its applications. *Sci. Rep.* **6**, 38028; doi: 10.1038/srep38028 (2016).

Publisher's note: Springer Nature remains neutral with regard to jurisdictional claims in published maps and institutional affiliations.



This work is licensed under a Creative Commons Attribution-NonCommercial-NoDerivs 4.0 International License. The images or other third party material in this article are included in the article's Creative Commons license, unless indicated otherwise in the credit line; if the material is not included under the Creative Commons license, users will need to obtain permission from the license holder to reproduce the material. To view a copy of this license, visit <http://creativecommons.org/licenses/by-nc-nd/4.0/>

© The Author(s) 2016